Differential regulation of myeloid leukemias by the bone marrow microenvironment

Daniela S. Krause[1,2,3,4], **Keertik Fulzele**[5], **Andre Catic**[1,2,3], **Chia Chi Sun**[6], **David Dombkowski**[4], **Michael P. Hurley**[1,2,3], **Sanon Lezeau**[1,2,3], **Eyal Attar**[7], **Joy Y. Wu**[5], **Herbert Y. Lin**[6], **Paola Divieti-Pajevic**[5], **Robert P. Hasserjian**[4], **Ernestina Schipani**[8], **Richard A. Van Etten**[9], and **David T. Scadden**[1,2,3,7]

[1]Center for Regenerative Medicine and Cancer Center, Massachusetts General Hospital, Boston, MA 02114

[2]Department of Stem Cell and Regenerative Biology, Harvard University, Cambridge, MA 02138

[3]Harvard Stem Cell Institute, Cambridge, MA 02138

[4]Department of Pathology, Massachusetts General Hospital, Boston, MA 02114

[5]Endocrine Unit, Massachusetts General Hospital, Boston, MA 02114

[6]Center for Systems Biology, Massachusetts General Hospital, Boston, MA 02114

[7]Division of Hematology/Oncology, Department of Medicine, Massachusetts General Hospital, Boston, MA 02114

[8]Indiana University School of Medicine, Indianapolis, IN 46202

[9]Molecular Oncology Research Institute, Tufts Medical Center, Boston, MA 02111

Abstract

Like their normal hematopoietic stem cell counterparts, leukemia stem cells (LSC) in chronic myelogenous leukemia (CML) and acute myeloid leukemia (AML) are presumed to reside in specific niches in the bone marrow microenvironment (BMM)[1], and may be the cause of relapse following chemotherapy.[2] Targeting the niche is a novel strategy to eliminate persistent and drug-resistant LSC. CD44[3,4] and IL-6[5] have been implicated previously in the LSC niche. Transforming growth factor (TGF)-β1 is released during bone remodeling[6] and plays a role in maintenance of CML LSCs[7], but a role for TGF-β1 from the BMM has not been defined. Here, we

Corresponding authors: David T. Scadden, M.D., Center for Regenerative Medicine and Cancer Center, Massachusetts General Hospital, 185 Cambridge Street, Boston, MA 02114, Phone: 617-724-5780, Fax: 617-724-2662, dscadden@mgh.harvard.edu. Richard A. Van Etten, M.D., Ph.D., Molecular Oncology Research Institute, Tufts Medical Center, 800 Washington St. Box 5609, Boston, MA 02111, Phone: 617-636-8110, Fax: 617-636-7060, rvanetten@tuftsmedicalcenter.org.

show that alteration of the BMM by osteoblastic cell-specific activation of the parathyroid hormone (PTH) receptor[8,9] attenuates *BCR-ABL1*-induced CML-like myeloproliferative neoplasia (MPN)[10] but enhances MLL-AF9-induced AML[11] in mouse transplantation models, possibly through opposing effects of increased TGF-β1 on the respective LSC. PTH treatment caused a 15-fold decrease in LSCs in wildtype mice with CML-like MPN, and reduced engraftment of immune deficient mice with primary human CML cells. These results demonstrate that LSC niches in chronic and acute myeloid leukemias are distinct, and suggest that modulation of the BMM by PTH may be a feasible strategy to reduce LSC, a prerequisite for the cure of CML.

Activation of osteoblastic cells in the bone marrow by PTH alters normal hematopoiesis[4]. We therefore tested whether PTH signaling could affect leukemogenesis by using transgenic mice with osteoblastic cell-specific expression of a constitutively active receptor for PTH and PTH-related peptide (PPR) under control of the 2.3 fragment of the collagen α1(I) promoter (Col1-caPPR mice)[8,9] or WT littermates as recipients in the retroviral transduction/transplantation model of CML-like MPN[12]. In Col1-caPPR recipients, the cumulative mortality due to BCR-ABL1-induced CML-like MPN was significantly decreased ($P < 0.001$; Fig. 1a) and overall survival significantly prolonged ($P = 0.002$, logrank test; Fig. 1b), with half of recipients succumbing to histiocytic sarcoma (HS), a BCR-ABL1-induced malignancy of monocyte-macrophages (Fig. 1b and Supplementary Fig. 1a–f) that can arise ~2 months after transplantation under conditions where efficiency of induction of CML-like MPN is low[12,13]. An equivalent number of proviral clones, representing leukemia-initiating cells[4], engrafted in WT and Col1-caPPR recipient spleen (Fig. 1c) and BM (Supplementary Fig. 1g), while homing of BCR-ABL1$^+$ c-Kit$^+$Lin$^-$ Sca-1$^+$ (KLS) cells to BM and spleen (Supplementary Fig. 1h) of Col1-caPPR or WT mice was not different. Yet, counts of circulating GFP$^+$ leukocytes remained normal in most Col1-caPPR recipients at a time (20d post-transplant) when leukocytosis was evident in WT recipients (data not shown, $P = 0.03$), whereas the absolute number of BM-derived BCR-ABL1$^+$ (GFP$^+$) KLS cells, defined previously as LSC in this CML model[14], was decreased in Col1-caPPR recipients at the time of morbidity or death (Fig. 1d, $P = 0.03$, *t*-test). Therefore, LSC engrafted but were not maintained in Col1-caPPR recipients.

Rates of LSC apoptosis did not differ (data not shown), but the frequency of cycling GFP$^+$c-Kit$^+$Lin$^-$ (KL) cells in Col1-caPPR recipients was significantly decreased (Fig. 1e and Supplementary Fig. 1i, $P < 0.001$, *t*-test), and the number of viable BM cells in leukemic Col1-caPPR recipients was significantly reduced (Fig. 1f, $P < 0.001$, *t*-test). *BCR-ABL1*-dependent myeloid colony formation[15] was also significantly reduced from Col1-caPPR-derived *BCR-ABL1*$^+$ BM (Fig. 1g, $P = 0.02$, *t*-test). The survival of secondary recipients of BM grafts from leukemic Col1-caPPR donors was significantly prolonged compared to recipients of WT BM grafts (Fig. 1h, $P = 0.04$, logrank test). Together, these results demonstrate that *BCR-ABL1*-induced CML-like disease is attenuated in Col1-caPPR mice due to decreased frequency, proliferation and maintenance of the phenotypic LSC and leukemic progenitor pool in the BMM.

We also transduced WT BM with retrovirus expressing *MLL-AF9*, the product of human t(9;11)$^+$ AML that induces aggressive AML in mice[11]. Interestingly, the survival of Col1-

caPPR recipients was significantly shorter than that of WT recipients (Fig. 1i, $P < 0.001$, logrank test). The number of engrafting proviral clones in spleen of Col1-caPPR recipients was significantly increased compared to WT recipients (5.4 ± 1.3 versus 3.0 ± 1.1, respectively; $P = 0.01$, t-test), with similar findings in BM (Fig. 1j). These results demonstrate that, in contrast to CML-like MPN, *MLL-AF9*-induced AML is accelerated in Col1-caPPR recipients, possibly due to an increased number of leukemic clones that engraft and persist in the Col1-caPPR BMM.

As the BMM of Col1-caPPR mice is characterized by increased osteoclasts and bone remodeling[8], we treated WT and Col1-caPPR recipients of *BCR-ABL1*-transduced WT BM with an Fc-fusion protein (OPG-Fc) of osteoprotegerin, a decoy receptor for RANKL that can reverse the bone phenotype in Col1-caPPR mice[16]. OPG-Fc treatment significantly increased the frequency of CML-like MPN in Col1-caPPR recipients from 40% to 90% (Fig. 2a and Supplementary Table 1; $P = 0.02$, Chi square test), although the increase in mortality in Col1-caPPR recipients treated with OPG-Fc did not reach statistical significance ($P = 0.06$, log-rank test; Supplementary Fig. 2a). Interestingly, treatment with the osteoclast inhibitor zolendronate did not restore CML-like MPN (data not shown), possibly due to the distinct mechanisms of OPG-Fc (RANKL antagonism) and zolendronate (inhibition of isoprenoid biosynthesis) on bone remodeling.

Anabolic effects of PTH on bone formation during bone remodeling are diminished in *Tgfb1*$^{-/-}$ mice[17]. Consistently, TGF-β1 protein (Fig. 2b) and biologically active TGF-β1 (Fig. 2c, $P = 0.02$, t-test) were increased in the bones of Col1-caPPR mice. Whereas TGF-β1$^+$ osteoblasts and osteoclasts are increased in Col1-caPPR recipients, OPG-Fc treatment eliminated these cells (Fig. 2d and Supplementary Fig. 2b) and significantly reduced nuclear pSMAD2/3, downstream of TGF-β receptor I (TGFβRI), in hematopoietic cells from WT and Col1-caPPR mice with CML ($P = 0.004$ and $P = 0.02$, respectively, t-test; Fig. 2e and Supplementary Fig. 2c). Whereas there was no direct effect of OPG-Fc on *BCR-ABL1*$^+$ cells in vitro (Supplementary Figs. 2d,e), we hypothesized that increased TGF-β1 signaling in the Col1-caPPR BMM might suppress CML progenitor growth, given that these cells have increased expression of TGFβRI compared to AML cells ($P = 0.027$, t-test, Supplementary Fig. 3a–c)[18,19]. Indeed, TGF-β1 significantly inhibited the in vitro growth of *BCR-ABL1*$^+$ K562 but not *MLL-AF9*$^+$ THP-1 cells (Fig. 2f), and direct intrafemoral injection of TGF-β1 in WT recipients with CML-like MPN dramatically reduced BM cellularity (Fig. 2g).

We further hypothesized that the LSC niche might differ between spleen and BM of Col1-caPPR recipients. In contrast to elevated TGF-β1 in Col1-caPPR bone, TGF-β1 levels in Col1-caPPR spleen were similar to those in WT spleen and bone (Fig. 2h). CML-like MPN could be induced in secondary recipients by transplantation of BM from WT or splenocytes from WT or Col1-caPPR primary leukemic mice, but not by Col1-caPPR BM (Fig. 2i). However, splenectomy of WT or Col1-caPPR primary recipients prior to transplanation of *BCR-ABL1*-transduced BM did not affect leukemic mortality (Supplementary Fig. 3d), suggesting differential maintenance of LSC in the BM versus spleen of Col1-caPPR mice, possibly due to different TGF-β1 levels in the respective niches. Taken together, these data support a model in which TGF-β1 generated by increased bone remodeling in Col1-caPPR mice suppresses *BCR-ABL1*-mediated MPN and may impair the maintenance of LSC.

To validate this, we assessed whether TGF-β1 blockade could increase the incidence of CML in Col1-caPPR recipients. Lentiviral shRNA knockdown of TGFβRI (to ~60% of control, Supplementary Fig. 4a) in *BCR-ABL1*-expressing cells accelerated the development (Fig. 3a*; P* = 0.007, logrank test) and increased the overall incidence (*P* = 0.04, Fisher's exact test; data not shown) of fatal CML-like MPN in Col1-caPPR recipients relative to control scrambled shRNA lentivirus. Conversely, overexpression of TGFβRI in *MLL-AF9*^{+} AML (Supplementary Fig. 4b) resulted in modest but significant prolongation of survival of Col1-caPPR recipients (Fig. 3b, *P* = 0.02, logrank and Wilcoxon tests). In response to TGF-β1, nuclear pSMAD2/3 was signficantly increased in CML LSCs compared to saline-treated cells (*P* = 0.01, *t*-test), whereas pSMAD2/3 staining was similar in AML LSCs with and without TGF-β1 treatment (Fig. 3c,d). As described previously for CML LSCs[7], staining for FoxO3a was predominantly nuclear with low pAKT staining (Supplementary Fig. 5a), while the percentage of CML LSC with nuclear pSMAD2/3 was significantly higher in Col1-caPPR than in WT mice (*P* = 0.02, *t*-test, Supplementary Fig. 5b). These data suggest that TGF-β1 derived from the BMM in Col1-caPPR recipients suppresses CML-like MPN, while *MLL-AF9*-induced AML is insensitive to this effect due in part to lack of TGFβRI expression and/or higher constitutive pSMAD2/3 signaling.

Treatment of WT Balb/c mice by continuous infusion of PTH prior to transplantation of *BCR-ABL1*-transduced BM caused a transient increase in blood calcium levels[20] (Supplementary Fig. 6a) and a reduction in splenomegaly (Supplementary Fig. 6b), but did not alter LSC engraftment (Supplementary Fig. 6c) or prolong overall survival (data not shown). However, PTH treatment significantly reduced the efficiency of transplantation of CML-like MPN to secondary recipients (Supplementary Fig. 6d,e), with limiting dilution analysis demonstrating a 15-fold reduction in BM LSC frequency (1 in 6.4×10^6 BM cells in PTH-treated versus 1 in 4.3×10^5 BM cells in saline-treated donors, *P* = 0.0006; Fig. 4a). This correlated with increased overall survival of all secondary recipients of BM from PTH-treated donors (*P*=0.03, Wilcoxon test; Fig. 4b), an effect observed in all cohorts except recipients of the lowest cell dose (Supplementary Fig. 6f). Treatment of WT mice with established CML-like MPN (Supplementary Fig. 7a,b) with imatinib alone or in combination with intermittent infusions of PTH resulted in similar prolongation in survival (Fig. 4c, *P*<0.0001 vs saline-treated controls), with long-term disease-free survival observed predominantly in the cohort treated with PTH + imatinib (33% vs 6% with imatinib alone). PTH treatment, alone or with imatinib, significantly decreased the percentage of cycling KL cells compared to imatinib monotherapy (Fig. 4d; *P* = 0.02 and *P* = 0.04, respectively, *t*-test).

To extend these results to human CML, we injected total BM cells (97–100% Ph[+] by FISH, data not shown) from seven untreated subjects with CML in chronic phase into NOD-SCID interleukin-2 receptor γc^{−/−} (NSG) recipient mice pretreated with saline or PTH. Engraftment of human CD45 leukocytes, assessed in BM aspirates by flow cytometry or estimated by levels of human β-glucuronidase transcripts as determined by qRT-PCR (Supplementary Fig. 7c), did not differ significantly between saline- and PTH-treated mice (0.2% to 4.8%, Fig. 4e, left panel). When results from recipients of different subject samples were pooled[21] to minimize the known variability of engraftment of human CML cells in

immunodeficient mice[22], PTH treatment was associated with a significant decrease in leukemic engraftment (Fig. 4e, right panel, P=0.049, t-test). These data suggest that modulation of the niche is also deleterious to human CML progenitors, and while conclusions from xenograft studies must be drawn with caution, the results provide some support for testing PTH in human subjects with CML.

In this report, we show that modulation of the BMM can alter the course of leukemia in a physiologically accurate and quantitative mouse model of human CML. We also provide evidence that the LSC niche in *MLL-AF9*^{+} AML is distinct from that in CML. Our data suggest that the beneficial effect of PTH in CML is mediated via suppressive effects of TGF-β1, secreted by a BMM characterized by increased bone turnover, on CML LSC, although we cannot exclude a role for other cytokines induced by PTH signaling. In contrast, the acceleration of *MLL-AF9*^{+} AML in Col1-caPPR mice may reflect decreased sensitivity to TGF-β1 or increased size of the niche for AML LSC. Our findings differ from those of Naka et al.[7], and this may reflect the known influence of dose and context on the effects of TGF-β1, with supraphysiologic levels of TGF-β1 mediating negative effects on CML LSC in our model. In conclusion, our results suggest that targeting the hematopoietic microenvironment through PTH may render it hostile for CML cells, raising the possibility of altering the tumor microenvironment as a novel and potentially complementary approach to tumor cell-specific therapeutics.

Online Methods

Mice

We purchased Balb/c and NOD SCID interleukin (IL)-2 receptor γ deficient (NSG) mice from Charles River Laboratories (Wilmington, MA) and Jackson Laboratory (Bar Harbor, ME), respectively.

BM transduction and transplantation

Alternatively to MSCV-IRES GFP BCR-ABL1, we also generated MSCV-IRES RFP BCR-ABL1 or MSCV-IRES RFP TGFβRI (cloned into the MSCV-IRES RFP vector as an EcoRI fragment) red fluorescent *BCR-ABL1*- or *TGFβRI* expressing retrovirus. For the generation of lentivirus expressing the TGFβRI-knockdown or scrambled short hairpin (sh) RNA, we transfected 293 cells with GIPZ scrambled or GIPZ RMM4431-99440663 shRNA (Open Biosystems, Huntsville, AL) and the genes encoding the envelope proteins 8.9 and VSV-G. We tested viral supernatants for efficient knockdown of *TGFβRI* by qPCR after infection of 3T3 fibroblasts, and assessed knockdown of TGFβR1 in leukemic cells by RT-qPCR of sorted GFP[+] (GIPZ[+] lentiviral vector) and RFP[+] (BCR-ABL1^{+}) cells. *TGFβRI*-specific primers were 5′-CAGCTCCTCATCGTGTTGGTG-3′ (forward) and 5′-GCCCCTGTTTTTGAAGATGGTG-3′ (reverse).

In homing assays, we transplanted 2.6×10^6 5-FU-treated, *BCR-ABL1*-transduced BM cells intravenously into 11 WT and 11 Col1-caPPR mice. 18 hours later, we analyzed BM and spleen cells of recipient mice from either genotype by flow cytometry for KLS cells and Annexin-positivity (Invitrogen, Grand Islan, NY) according to the manufacturer's instructions.

For xenotransplantation, we intravenously injected $11–50 \times 10^6$ frozen total BM cells from 7 different untreated subjects with CML in chronic phase into one to two irradiated (300 cGy) saline- and one to two irradiated PTH-treated NSG mice per CML subject. Prior fluorescence in-situ hybridization revealed positivity for the *BCR-ABL1* translocation in >95% of cells. Saline- and PTH-treatment by osmotic minipump, as described below, was initiated 4 weeks prior to xenotransplantation and was continued for 14 weeks thereafter.

In the secondary transplant experiments in the FVB/Col1-caPPR background, we injected 2.5×10^6 BM or spleen cells from WT FVB or Col1-caPPR mice on day 19 after primary transplantation with *BCR-ABL1*$^+$ cells into WT recipients. Flow cytometric analysis of PB before harvesting of BM and spleen cells of donor animals revealed fully established CML-like MPN in all donors with a range of 9.9–20.9% CD11b$^+$ GFP$^+$ cells in the WT donor mice and a range of 19.6–37.7% CD11b$^+$ GFP$^+$ cells in the Col1-caPPR donor mice. We transplanted BM or spleen grafts from 16 or 10 different, individual donors per FVB WT or Col1-caPPR donor group, respectively, into four recipients each, two of which received a BM and two a spleen graft.

For the secondary transplantation in the Balb/c background (limiting dilution experiment), we treated primary WT Balb/c mice with saline versus human PTH (1–34) via osmotic minipump for 4 weeks prior to transplantation with *BCR-ABL1*$^+$ cells. Upon full establishment of CML on day 17, we harvested BM from 5 saline- versus 5 PTH-treated primary animals and pooled the BM within one treatment group. We then transplanted BM from a saline- versus a PTH-treated BM environment in limiting dilution of 2×10^6, 10^6, 7×10^5, 2×10^5, 7×10^4 and 2×10^4 cells into 5 recipients each.

Southern blot analysis

We digested genomic DNA from BM or spleen of leukemic WT or Col1-caPPR mice with Bgl II, transferred to Nylon membranes and hybridized with a radioactively labeled probe from the GFP gene, in order to detect distinct proviral integration sites. Single copy DNA represents control DNA from a cell line that contains a single *BCR-ABL1* provirus.

TGF-β1 luciferase assay

We transiently transfected Hep3B cells with a TGF-β1-responsive luciferase promoter (CAGA-luc) and a transfection control *Renilla* luciferase (pRL-TK) vector with Lipofectamine 2000. Forty-eight hours after transfection, cells were serum starved in 1% FBS Optimem I and then incubated for 16 hours with the supernatants from crushed bones from WT or Col-1caPPR mice. As negative and positive controls, cells were incubated with either PBS or 5 ng/ml TGF-β1 (R&D systems). Experiments were performed in triplicate. Subsequently, we lysed the cells and measured luciferase reporter activity by Dual Reporter Assay (Promega), as described[23]. We determined relative luciferase activity as the ratio of Luciferase units to *Renilla*.

Splenectomy

7 days before transplantation, we anesthesized mice and made an incision below the left ribcage. We then incised the peritoneum aseptically and grasped the spleen. We tied off

splenic vessels securely and removed the spleen, subsequently suturing the the peritoneum and skin.

Analysis of diseased mice

We diagnosed the different *BCR-ABL1*-associated diseases in this mouse model, namely CML-like MPN, B-cell acute lymphoblastic leukemia (B-ALL) or HS and MLL-AF9-induced AML, based on clinicopathological criteria, as described[4,11,12]. We assessed the leukemic burden in diseased animals weekly by a Vetscan 5 HM (Abaxis, Union City, California) complete blood count analyzer and by staining leukocytes from PB with a phycoerythrin (PE)-conjugated antibody to CD11b (myeloid cells) (Biolegend, San Diego, CA) in CML-like MPN, a PE-conjugated antibody to BP-1 (BD Biosciences, San Jose, CA) in the case of B-ALL or an allophycocyanin-conjugated antibody to CD11b (BD Biosciences, San Jose, CA) and a PE-conjugated antibody to Gr-1 (eBioscience, San Diego, CA) in the case of AML and analysing for expression of GFP. We also stained leukocytes with an antibody to TGFβRI (Millipore, Billerica, MA, USA) and a secondary PE-conjugated anti-rabbit-IgG antibody.

By flow cytometry we analysed BM aspirates, which we obtained as described[4], for expression of GFP, Mac-1, Gr-1, lineage (B220, CD5, Gr-1 and Ter119), c-Kit and Sca-1 and for cycling status by Hoechst 33342 (37 C for 30 minutes) staining on a BD LSRII (Becton Dickinson). We measured cell viability by trypan blue-staining and counting of live cells on a Cellometer Vision (Nexcelom Bioscience LLC, Lawrence, MA).

We assessed engraftment of human cells in NSG mice by flow cytometry using anti-human CD45 (BD Biosciences, Franklin Lakes, NJ). Human hematopoietic engraftment was also measured by quantitative reverse-transcriptase polymerase chain reaction (qRT-PCR) for human beta-glucuronidase (GUS) transcripts (forward primer: 5′-GTCTGCGGCATTTTGTCGG-3′, reverse primer: 5′-ACCTCCCGTTCGTACCACA-3′); a standard curve relating human CD45 expression to human GUS transcripts was used to estimate % human engraftment for those samples where hCD45 was not measured directly. To quantify leukemic engraftment, we performed qRT-PCR for *BCR-ABL1* using 5′-GTGCAGAGTGGAGGGAGAAC-3′ (forward) and 5′-ATGCTACTGGCCGCTGAA-3′ (reverse) primers, and used these data to estimate the percentage of *BCR-ABL1*^{+} cells based on a standard curve (Supplementary Fig. 7).

For assessment of the incidence of CML in different transplants, we used the following criteria to define CML: Primary transplants: WBC >15,000/ul and >4% GFP[+] Mac-1^{+} cells in PB or death due to CML (hepatosplenomegaly and pulmonary congestion and hemorrhages), secondary transplants: WBC >10,000/ul or >1% GFP[+] Mac-1^{+} cells in PB. We defined AML by the presence of Gr-1^{+} GFP[+] myeloid blasts in the PB and massive infiltration of the liver and spleen by these cells.

Histopathology of diseased mice

We took tissue samples of lung, liver, spleen and bone from every deceased mouse and processed, embedded, sectioned and stained them with hematoxylin & eosin for

histopathological analysis or subjected to immunohistochemistry analysis for TGF-β1 (Abcam, Cambridge, MA) following standard procedures. We decalcified bones in 0.5 M EDTA. We performed tartrate-resistant acid phosphatase (TRAP) staining on bones from the osteoprotegerin-experiment using 50mM tartrate in acetate buffer and TRAP reagent in N,N-dimethylformamide, with counterstaining performed with methyl green.

A blinded pathologist counted the percentage of hematopoietic cells positive for pSMAD2/3.

Drug treatment

We injected 3 mg/kg of rat or human osteoprotegerin-Fc (OPG-Fc) chimera (from Dr. Ernestina Schipani) subcutaneously every other day (three times a week) as described[16] beginning 1 week prior to tranplantation. We implanted osmotic minipumps (Alzet, Cupertino, CA) as described by the manufacturer. We filled the pumps the previous day with either saline or PTH (resuspended as described[20]) to allow a daily dose of 80 μg/kg for a total of 14 days and left them in sterile saline at 37 C overnight, and changed pumps every two weeks. We initiated treatment 4 weeks before transplantation and continued until the animal's death.

For the daily subcutaneous injections (intermittent dosing regimen), we administered human PTH (1–34) or saline at 80 μg/kg/d. We crushed a 100 mg tablet of imatinib, resuspended it in saline, spun, filtered and subcutaneously injected this daily, beginning on day 10 after transplantation.

We performed intrafemoral injections with PBS (left femur) or 250 ng TGF-β1 (right femur) (Sigma-Aldrich, St. Louis, MO) daily on days 15–18 after transplantation of *BCR-ABL1-* transduced BM into WT FVB recipients.

Western Blotting

We crushed and filtered bones or the spleen of a mouse, and prepared lysates in RIPA buffer (50mM Tris Hcl pH7.4, 150mM NaCl, 1% Triton X-100, 1% NaDOC, 0.1% SDS, 1mM EDTA), 50mM NaF, 1mM Na_3VO_4, aprotinin and PMSF. Before loading, we measured the total protein content of lysates by the Bradford dye-binding method (Bio-Rad, Hercules, CA), equalized samples for protein content and boiled them in sample buffer containing DTT. We blotted the proteins onto a PVDF membrane and probed with an antibody to TGF-β1 (Abcam, Cambridge, MA). We then reprobed the membrane with an antibody to actin (Santa Cruz, Santa Cruz, CA). We quantified Western blots by ImageJ software by forming the ratio between expression levels of TGF-β1 and the sample's respective actin control.

In vitro assays

We plated K562 or *MLL-AF9*^{+} THP-1 cells in sixplicate at 100,000 cells per well of a 6-well plate in RPMI with 5ng/ml TGF-β1 or vehicle. In a separate experiment, we incubated 10^5 K562 cells with 130 ng/ml OPG-Fc or saline, as described[24], and assessed daily for cell number and viability.

For the methylcellulose colony assays, we plated 2×10^4 total BM or 2×10^5 spleen cells from WT or Col1-caPPR recipients of *BCR-ABL1*^{+}-transduced BM on day 21 after transplantation in triplicate in cytokine-free methylcellulose (M3231, Stem Cell Technologies, Vancouver, Canada) supplemented with 100 pg/ml IL-3 (Peprotech, Rocky Hill, NJ). We scored colonies after 10 days. We used serial replating assays in methylcellulose (M3434) for generation of *MLL-AF9*^{+} immortalized colony-forming cells for immunofluorescence studies, as described[25].

Immunofluorescence

We prepared cytospin preparations of *BCR-ABL1*^{+} or *MLL-AF9*^{+} KLS or lineage negative cells, respectively, on poly-L-lysine covered glass coverslips and stained them for immunofluorescence analysis with anti-pSMAD 2/3, pAkt (Cell Signaling, Danvers, MA) and Foxo3a (Sigma, St. Louis, MO), with secondary antibody staining by anti-rabbit Alexa Fluor 647 (Invitrogen, Grand Island, NY), as described[7]. We visualized the cells by a Nikon Eclipse T*i* confocal laser microscope and individually quantitated by ImageJ software.

Serum calcium measurement

We added plasma to the calcium-detection agent and measured total calcium concentration of PB according to the manufacturer's instructions (Stanbio Laboratory, Boerne, TX).

Additional statistical Methods

We determined the statistical significance of the incidence of CML or survival rates in different treatment groups by Fisher's Exact or Chi-square test. We used L-Calc software (Stemcell Technologies, Vancouver, Canada) to calculate LSC frequency by Poisson statistics.

Supplementary Material

Refer to Web version on PubMed Central for supplementary material.

Acknowledgments

References

1. Ishikawa F, et al. Chemotherapy-resistant human AML stem cells home to and engraft within the bone-marrow endosteal region. Nat Biotechnol. 2007; 25:1315–1321. [PubMed: 17952057]

2. Krause DS, Van Etten RA. Right on target: eradicating leukemic stem cells. Trends Mol Med. 2007; 13:470–481. [PubMed: 17981087]

3. Jin L, Hope KJ, Zhai Q, Smadja-Joffe F, Dick JE. Targeting of CD44 eradicates human acute myeloid leukemic stem cells. Nat Med. 2006; 12:1167. [PubMed: 16998484]

4. Krause DS, Lazarides K, von Andrian UH, Van Etten RA. Requirement for CD44 in homing and engraftment of BCR-ABL-expressing leukemic stem cells. Nat Med. 2006; 12:1175–1180. [PubMed: 16998483]

5. Reynaud D, et al. IL-6 controls leukemic mutipotent progenitor cell fate and contributes to chronic myelogenous leukemia development. Cancer Cell. 2011; 20:661–673. [PubMed: 22094259]

6. Tang Y, et al. TGF-beta1-induced migration of bone mesenchymal stem cells couples bone resorption with formation. Nat Med. 2009; 15:757–765. [PubMed: 19584867]

7. Naka K, et al. TGF-beta-FOXO signalling maintains leukaemia-initiating cells in chronic myeloid leukemia. Nature. 2010; 463:676–680. [PubMed: 20130650]

8. Calvi LM, et al. Activated parathyroid hormone/parathyroid hormone-related protein receptor in osteoblastic cells differentially affects cortical and trabecular bone. J Clin Invest. 2001; 107:277–286. [PubMed: 11160151]

9. Calvi LM, et al. Osteoblastic cells regulate the haematopoietic stem cell niche. Nature. 2003; 425:841–846. [PubMed: 14574413]

10. Daley GQ, Van Etten RA, Baltimore D. Induction of chronic myelogenous leukemia in mice by the P210$^{bcr/abl}$ gene of the Philadelphia chromosome. Science. 1990; 247:824–830. [PubMed: 2406902]

11. Krivtsov AV, et al. Transformation from committed progenitor to leukaemia stem cell initiated by MLL-AF9. Nature. 2006; 442:818–822. [PubMed: 16862118]

12. Li S, Ilaria RL, Million RP, Daley GQ, Van Etten RA. The P190, P210, and P230 forms of the *BCR/ABL* oncogene induce a similar chronic myeloid leukemia-like syndrome in mice but have different lymphoid leukemogenic activity. J Exp Med. 1999; 189:1399–1412. [PubMed: 10224280]

13. Li S, et al. Interleukin-3 and granulocyte-macrophage colony-stimulating factor are not required for induction of chronic myeloid leukemia-like myeloproliferative disease in mice by *BCR/ABL*. Blood. 2001; 97:1442–1450. [PubMed: 11222392]

14. Hu Y, et al. Targeting multiple kinase pathways in leukemic progenitors and stem cells is essential for improved treatment of Ph+ leukemia in mice. Proc Natl Acad Sci U S A. 2006; 103:16870–16875. [PubMed: 17077147]

15. Gishizky ML, Witte ON. Initiation of deregulated growth of multipotent progenitor cells by *bcr-abl* in vitro. Science. 1992; 256:836–839. [PubMed: 1375394]

16. Ohishi M, et al. Osteoprotegerin abrogated cortical porosity and bone marrow fibrosis in a mouse model of constitutive activation of the PTH/PTHrP receptor. Am J Pathol. 2009; 174:2160–2171. [PubMed: 19389927]

17. Wu X, et al. Inhibition of Sca-1-positive skeletal stem cell recruitment by alendronate blunts the anabolic effects of parathyroid hormone on bone remodeling. Cell Stem Cell. 2010; 7:571–180. [PubMed: 21040899]

18. Haferlach T, et al. Clinical utility of microarray-based gene expression profiling in the diagnosis and subclassification of leukemia: report from the International Microarray Innovation in Leukemia Study Group. J Clin Oncol. 2010; 28:2529–2537. [PubMed: 20406941]

19. Radich JP, et al. Gene expression changes associated with progression and response in chronic myeloid leukemia. Proc Natl Acad Sci U S A. 2006; 103:2794–2799. [PubMed: 16477019]

20. Guo J, et al. Suppression of Wnt signaling by Dkk1 attenuates PTH-mediated stromal cell response and new bone formation. Cell Metab. 2010; 11:161–171. [PubMed: 20142103]

21. Heaney NB, et al. Bortezomib induces apoptosis in primitive chronic myeloid leukemia cells including LTC-IC and NOD/SCID repopulating cells. Blood. 2010; 115:2241–2250. [PubMed: 20068223]

22. Wang JCY, et al. High level engraftment of NOD/SCID mice by primitive normal and leukemic hematopoietic cells from patients with chronic myeloid leukemia in chronic phase. Blood. 1998; 91:2406–2414. [PubMed: 9516140]

23. Babitt JL, et al. Bone morphogenetic protein signaling by hemojuvelin regulates hepcidin expression. Nat Genet. 2006; 38:531–539. [PubMed: 16604073]

24. Burgess TL, et al. The ligand for osteoprotegerin (OPGL) directly activates mature osteoclasts. J Cell Bio. 1999; 145:527–538. [PubMed: 10225954]
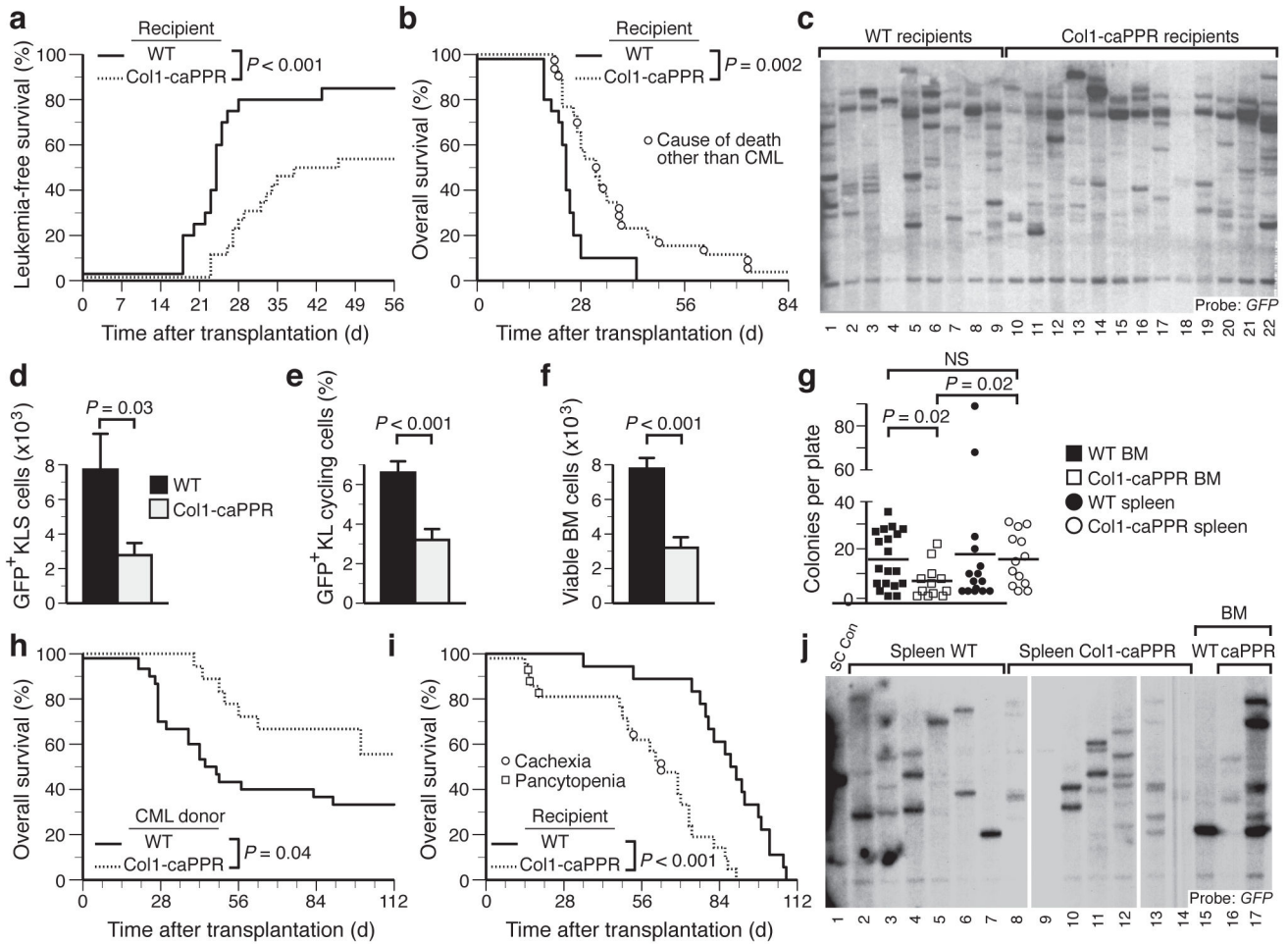
25. Somervaille TCP, Cleary ML. Identification and chracterization of leukemia stem cells in murine MLL-AF9 acute myeloid leukemia. Cancer Cell. 2006; 10:257–268. [PubMed: 17045204]

Figure 1.
BCR-ABL1-induced CML-like MPN is attenuated in Col1-caPPR recipients. (**a** and **b**) Cumulative mortality from CML-like MPN (**a**) and overall survival (**b**) for WT (n=20, solid) or Col1-caPPR (n=26, dashed) recipients of *BCR-ABL1*-transduced WT BM (*P*< 0.001 and *P* = 0.002, respectively; logrank tests). (**c**) Disease clonality in spleens of WT (lanes 1–9) and Col1-caPPR (lanes 10–22) recipients (WT, 6.6±2.1 clones; Col1-caPPR, 7.2±2.1 clones; *P* = 0.52, *t*-test). (**d**) Absolute number of GFP[+] (*BCR-ABL1*^{+}) KLS cells in the BM of Col1-caPPR mice (*P* = 0.03, *t*-test, gray bar, n=20) versus WT mice (black bar, n=20). (**e**) Hoechst[+] *BCR-ABL1*^{+} cycling c-Kit[+]Lin^{−} cells in the BM of Col1-caPPR (gray) mice compared to WT mice (black) (*P* < 0.001, *t*-test). (**f**) Absolute number of viable BM cells from Col1-caPPR (gray) versus WT (black) recipients of *BCR-ABL1*-transduced BM (*P* < 0.001, *t*-test). (**g**) Number of colonies in methylcellulose from BM cells (squares) from Col1-caPPR (open squares) or WT (solid squares) mice with CML-like MPN (*P* = 0.02, *t*-test) and from spleen cells (circles) from Col1-caPPR (open circles) or WT (solid circles) mice with CML-like MPN (*P* = 0.02, *t*-test). (**h**) Overall survival for WT secondary recipients of *BCR-ABL1*^{+} BM grafts from a WT (solid, n=30), compared to a Col1-caPPR (dashed, n=18) microenvironment (*P* = 0.04). (**i**) Survival curves for WT (n=18, solid) or Col1-caPPR (n=21, dashed) recipients of *MLL-AF9*-transduced WT donor BM (*P* < 0.0001,

logrank test). (**j**) Clonality of *MLL-AF9*^{+} AML-like disease in spleen of WT recipients (lanes 2–7) compared to spleen of Col1-caPPR recipients (lanes 8–14) ($P = 0.01$, *t*-test) and in BM of WT (lane 15) or Col1-caPPR recipients of *MLL-AF9*-transduced WT BM (lanes 16–17).
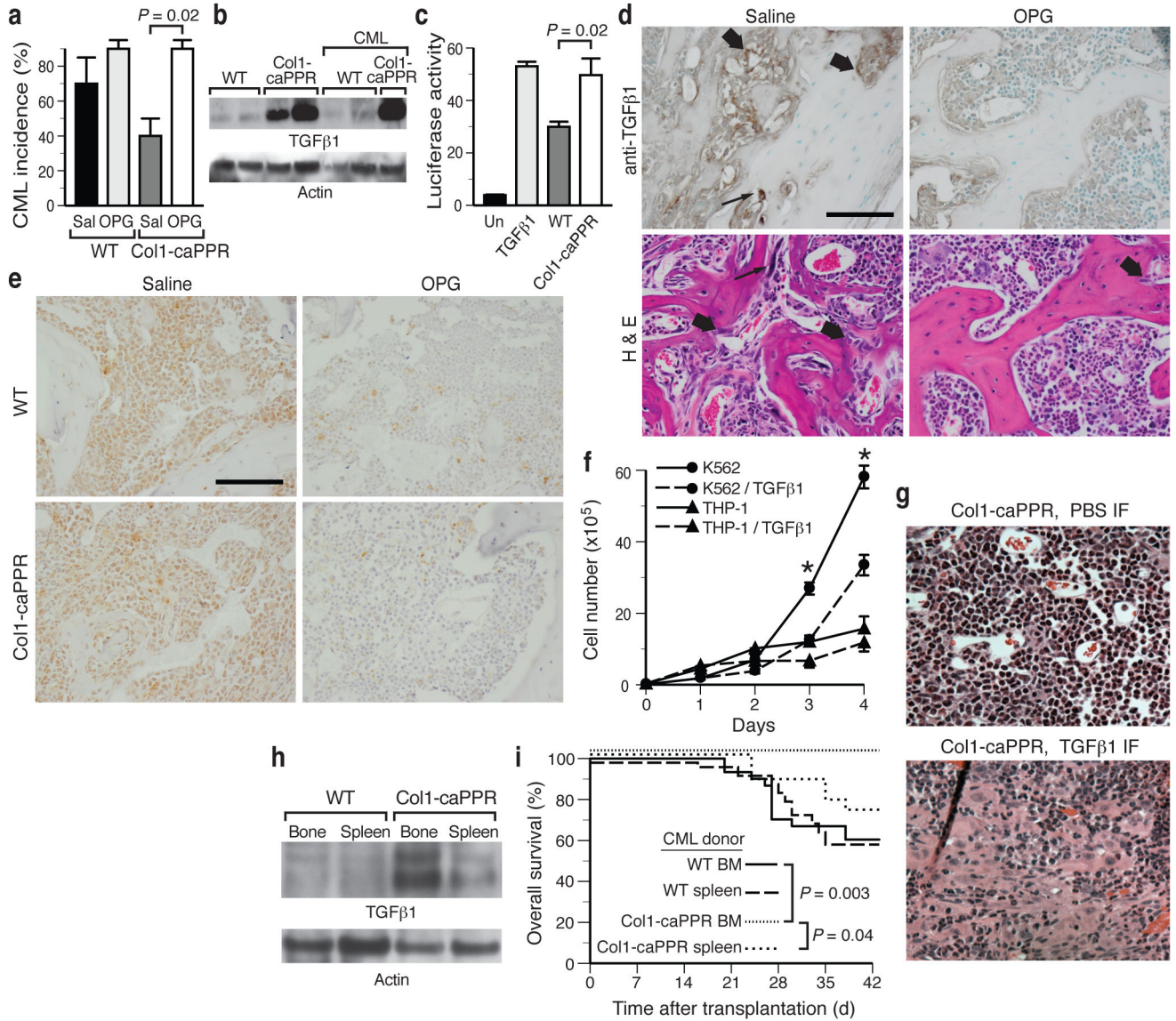
Figure 2.
TGF-β1 signaling is increased in the bones of Col1-caPPR mice and suppresses the growth
of *BCR-ABL1*^{+} cells in vitro. (**a**) Incidence of CML-like MPN in WT (left) and Col1-caPPR
(right) mice treated with osteoprotegerin (WT: light gray, Col1-caPPR: white, n=10) or
saline (wt: black, Col1-caPPR: dark gray, n=10) (P = 0.02, Chi-square). (**b**) Immunoblotting
of lysates from crushed bone from WT or Col1-caPPR mice probed with antibodies to TGF-
β1 (molecular mass 25 kDa) or actin (42 kDa) (mean intensity of TGF-β1 bands normalized
to actin control: WT, 0.6±0.2; Col1-caPPR, 2.5±0.3; P < 0.001, t-test) (**c**) Bioactive TGF-β1
in Col1-caPPR bones (white bar, n=8) compared to WT bones (dark gray bar, n=9) (P =
0.02, t-test). (**d**) Immunohistochemistry (top) for TGF-β1 and hematoxylin & eosin stains
(bottom) (Scale bar indicates 100 μm) on bones of Col1-caPPR mice with CML-like MPN
treated with saline (left) or OPG-Fc (right). The arrows depict TGF-β1^{+} osteoblastic cells
(bold arrow) and osteoclasts (thin arrow). (**e**) Immunohistochemistry (Scale bar indicates

100 μm) for pSMAD2/3 (detected by immunoperoxidase using yellow/brown horseradish-peroxidase chromogen) on bones of representative Col1-caPPR mice (bottom) with CML-like MPN treated with saline (left) or OPG-Fc (right). (**f**) Growth of *BCR-ABL1*⁺ K562 (circles) and *MLL-AF9*⁺ THP-1 (triangles) cells in the presence of vehicle (solid line) or TGF-β1 (dashed line); the differences in cell number at day 3 and 4 were significant ($P <$ 0.001, *t*-tests). (**g**) Hematoxylin-eosin-stained sections of BM of a representative (n=3) WT mouse with CML-like MPN treated by intrafemoral injections with PBS (left panel) or TGF-β1 (right panel) (Scale bar indicates 100 μm). (**h**) Immunoblotting of lysates from crushed bone or spleen from WT or Col1-caPPR mice with CML-like MPN probed with an antibody to TGF-β1 as in **b.** (**i**) Overall survival of WT secondary recipients of *BCR-ABL1*⁺ BM or spleen grafts from a WT (BM: solid, n=30; spleen: long dashes, n=24), compared to a Col1-caPPR (BM: dots, n=18; spleen: short dashes, n=20) microenvironment. Significant differences in survival (logrank tests) are indicated.
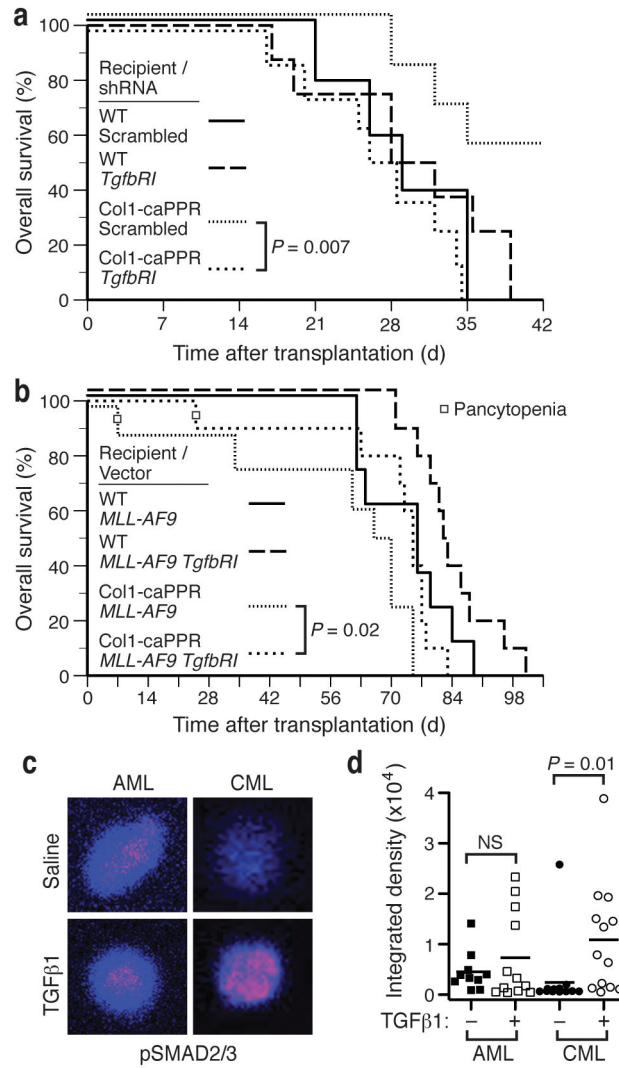
Figure 3.
Modulation of TGFβRI on leukemic cells differentially affects *BCR-ABL1*^{+} (chronic) and *MLL-AF9*^{+} (acute) myeloid neoplasms in a Col1-caPPR microenvironment. (**a**) Survival curves for WT or Col1-caPPR recipients of *BCR-ABL1*-transduced WT BM that was co-transduced with lentivirus expressing either scrambled shRNA (WT: solid line; Col1-caPPR: dotted line) or *Tgfbr1* shRNA (WT: long dashes; Col1-caPPR: short dashes). Survival of Col1-caPPR recipients of *BCR-ABL1*^{+} *Tgfbr1* shRNA[+] BM was significantly shortened (*P* = 0.007, logrank test) compared to Col1-caPPR recipients of *BCR-ABL1*^{+} scrambled shRNA[+] BM. All Col1-caPPR recipients of *BCR-ABL1*^{+} *Tgfbr1* shRNA[+] BM succumbed to CML-like MPN. (**b**) Survival curves for WT or Col1-caPPR recipients of WT BM transduced with *MLL-AF9* retrovirus alone (WT: solid line; Col1-caPPR: dotted line) or co-transduced with a retrovirus expressing TGFβRI (WT: long dashes; Col1-caPPR: short dashes). Survival of Col1-caPPR recipients of MLL-AF9^{+} TGFβRI[+] BM (n=10) was significantly prolonged (*P* = 0.02, logrank test) compared to Col1-caPPR recipients of BM transduced with *MLL-AF9* only (n=8). (**c**) pSMAD2/3 immunofluorescence staining of Lin[−] *MLL-AF9*^{+} (left) or *BCR-*

ABL1^{+} KLS cells treated *in vitro* with 5 ng/ml TGF-β1 (bottom) or saline (top). (**d**) Quantitation of individual cells from **c** by confocal microscopy. pSMAD2/3 staining was significantly increased in CML-initiating cells treated with TGF-β1 compared to saline-treated cells ($P = 0.01$, *t*-test), but not in AML-initiating cells.
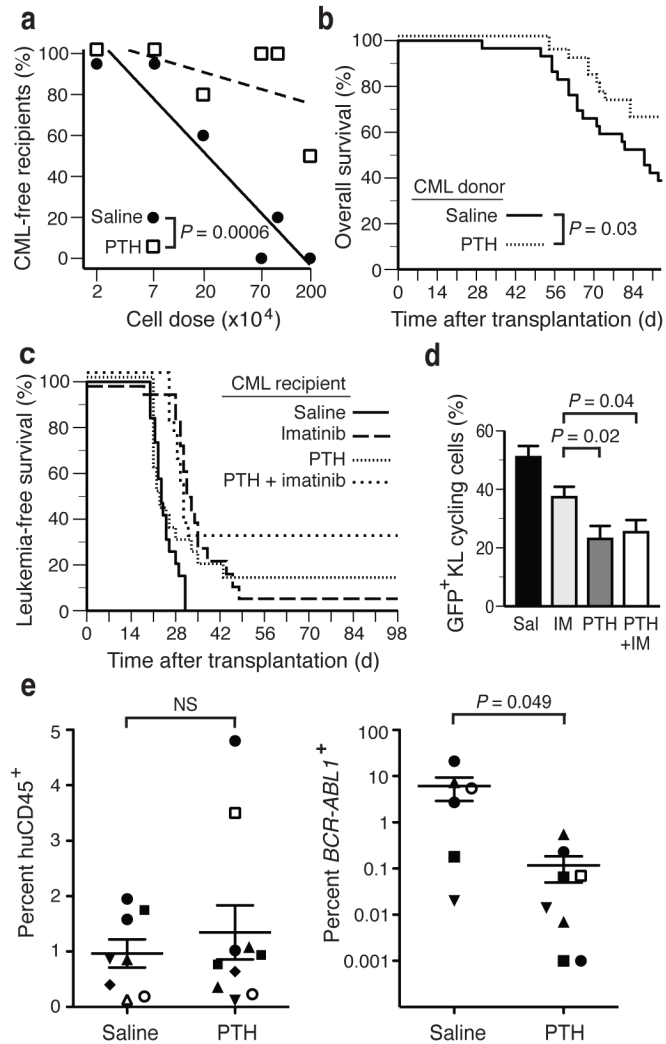
Figure 4.
PTH treatment reduces leukemia burden and LSC abundance in wt mice and leads to more longterm survivors in combination with imatinib. (**a**) Frequency of leukemia-free untreated secondary recipients of *BCR-ABL1*^{+} BM from saline- (black circles) or PTH- (open squares) treated donors in relation to the dose of transplanted bone marrow. The lines fitted by regression analysis (L-Calc) allow estimation of leukemia-initiating cell frequency, which was significantly lower in recipients of BM from PTH-treated donors ($P = 0.0006$). (**b**) Overall survival of WT secondary recipients of *BCR-ABL1*^{+} BM grafts from WT mice treated with PTH (dotted line, n=27) compared to WT mice treated with saline (solid line, n=29) ($P = 0.03$, logrank test). (**c**) Overall survival of WT recipients of *BCR-ABL1*-transduced BM treated with daily subcutaneous injections of saline (solid line, n=19) or PTH (dotted line, n=19), imatinib (long dashes, n=18) or a combination of PTH and imatinib (short dashes, n=18), randomized prior to transplantation. (**d**) Percentage of cycling GFP[+]c-Kit[+]Lin^{−} cells is significantly decreased in animals treated with PTH with or without imatinib ($P = 0.04$, *t*-test) compared to imatinib alone. (**e**) Levels (mean and s.d.) of human hematopoietic engraftment (measured or estimated percentage of hCD45^{+} leukocytes, left

panel) or BCR-ABL1^{+} engraftment (estimated by levels of *BCR-ABL1* transcripts, right panel) in BM aspirates from individual NSG recipients of primary human CML subject samples (n=7) that were treated with either saline or PTH ($P = 0.049$, *t*-test). Recipients of BM grafts from the same CML subject sample are indicated by the individual symbols. The two samples in the PTH-treated cohort at the bottom of the plot had *BCR-ABL1* transcript levels that were below the level of detection (estimated <0.001%) despite detectable levels of human cell engraftment.